406–420 *Nucleic Acids Research, 2019, Vol. 47, No. 1* *Published online 8 November 2018*
doi: 10.1093/nar/gky1083

Ribosomal protein eL24, involved in two intersubunit bridges, stimulates translation initiation and elongation

Ivan Kisly, Jaanus Remme* and Tiina Tamm*

Institute of Molecular and Cell Biology, University of Tartu, Tartu 51010, Estonia

Received May 18, 2018; Revised October 02, 2018; Editorial Decision October 15, 2018; Accepted October 19, 2018

ABSTRACT

Interactions between subunits in the *Saccharomyces cerevisiae* ribosome are mediated by universal and eukaryote-specific intersubunit bridges. Universal bridges are positioned close to the ribosomal functional centers, while eukaryote-specific bridges are mainly located on the periphery of the ribosome. Two bridges, eB13 and B6, are formed by the ribosomal protein eL24. The eukaryotic eL24 is composed of an N-terminal domain, a linker region and a C-terminal α-helix. Here, the functions of different domains of eL24 in the *S. cerevisiae* ribosome were evaluated. The C-terminal domain and the linker region of the eL24 form eukaryote-specific eB13 bridge. Phenotypic characterization of the eL24 deletion mutants indicated that the functional integrity of the eB13 bridge mainly depends on the protein–protein contacts between eL24 and eS6. Further investigation showed importance of the eB13 bridge in the subunit joining *in vivo* and *in vitro*. *In vitro* translation assay demonstrated the role of the eB13 bridge in both initiation and elongation steps of translation. Intriguingly, results of *in vitro* translation experiment suggest involvement of the N-terminal domain of eL24 in the translation initiation. Therefore, eL24 performs number of tasks required for the optimal ribosome functionality.

INTRODUCTION

Protein synthesis and ribosome biogenesis are the most energy-consuming processes in the cells (1–3). Numerous reports have shown that alterations in these processes caused by mutations in ribosomal proteins or biogenesis/translation factors affect efficiency of protein synthesis and lead to a variety of developmental disorders, ribosomopathies and cancer (3–7). Thus, integrity of ribosome, its individual components and other factors involved in translation is crucial for normal physiology of cells.

All main steps of protein synthesis—initiation, elongation, termination and ribosome recycling—depend on conformational changes of 80S ribosomes. Structural studies of prokaryotic and eukaryotic ribosomes point to ribosomal intersubunit bridges as important supporters of correct 50S/60S and 30S/40S subunits joining and rotation (8–11). The number and complexity of these bridges varies strongly across different domains of life and even within a single domain (10–12). However, comparison of bacterial, archaeal and eukaryotic ribosomes reveals universally conserved bridges at the core of ribosomes. These bridges contribute to the ribosomal functional centers and involve rRNA–rRNA, protein–rRNA and protein–protein type contacts (10–14). For example, in *Saccharomyces cerevisiae* ribosome twelve conserved bridges between 60S and 40S subunits have been determined (11).

The increased interaction surface between the subunits of eukaryotic ribosome, in comparison to the prokaryotic ribosome, is additionally regulated by eukaryote-specific bridges (10,11,13). These bridges lack rRNA–rRNA type interactions and are significantly predominated by protein components. The important part in eukaryote-specific bridges is assigned to eukaryote-specific rRNA expansion segments and eukaryote-specific protein domains/proteins. Both *S. cerevisiae* and *Homo sapiens* ribosomes contain five eukaryote-specific bridges (11,13). Bridges eB8, eB11, eB12 and eB13 are positioned on the periphery of ribosomal subunits exhibiting highest dynamics during translocation (11,13). Bridges eB12 and eB13 are structurally similar to each other. Both bridges are formed by the long C-terminal α-helices of proteins eL19 and eL24 that extend from 60S subunit E- and A-site sides, respectively (11). The fifth eukaryote-specific bridge, eB14, appears close to the decoding center and is formed by a 25 aa residues long protein eL41 (11). Several functional studies have suggested that eukaryote-specific intersubunit bridges and their components are important for the optimal ribosomal functionality (15–17).

*To whom correspondence should be addressed. Tel: +372 7375037; Email: ttamm@ut.ee
Correspondence may also be addressed to Jaanus Remme. Riia 23B, Tartu 51010, Estonia. Tel: +372 7375031; Email: jremme@ut.ee

In *S. cerevisiae* ribosome, two intersubunit bridges, eB13 and B6, are formed by the ribosomal protein eL24 (Figure 1, Supplementary Figure S1, Table 1) (11). Eukaryote-specific eB13 consists of multiple interactions of 60S subunit proteins eL24 and uL3 with 40S subunit protein eS6 and 18S rRNA. In the post-translocational state the core part of this bridge is formed by 11 contacts between C-terminal α-helix and linker region of eL24 and eS6. These interactions are accompanied by 10 contacts of eL24 with 18S rRNA helices 6, 10 and 44, and also by two contacts of uL3 with eS6 (Supplementary Figure S1, Table 1). Conserved intersubunit bridge B6 is made up of only two contacts: R43 and R47 located in the N-terminal domain of eL24 interact with G1670 and U1724 of 18S rRNA helix 44 (Supplementary Figure S1, Table 1) (11).

Yeast eL24 is one out of 14 nonessential ribosomal proteins (18). This 155 aa residues long protein is encoded by two paralogous genes *RPL24A* and *RPL24B*. Proteins encoded by these genes differ only in five amino acid residues. Analysis of *rpl24AΔ* and *rpl24BΔ* mutants suggested that expression of paralog A plays a more important role for cell growth than paralog B (19). There is no bacterial homolog of eL24, while archaea express shortened version of eL24 lacking linker region and C-terminal α-helix (20). eL24 is known to be one of the last proteins incorporated into 60S subunit at the cytoplasmic step of maturation, along with uL10/P0 and uL16/L10 (21–23). It is also known that the N-terminal domain of eL24 is homologous to the N-terminal domain of essential 60S subunit biogenesis factor Rlp24, associated with pre-60S particle during nucleolar, nuclear and cytoplasmic steps of maturation (23). Rlp24 is an important docking factor for other ribosome biogenesis factors and is required for processing of the internal transcribed spacer 2 (ITS2) in 27SB pre-rRNAs (23). AAA-ATPase Drg1 removes Rlp24 from 60S subunit at the cytoplasmic step of maturation, which is followed by incorporation of eL24, so eL24 and Rlp24 may share the same binding site on the ribosome (21,23). Although eL24 is dispensable for cell viability, lack of it results in reduced cell growth rate by 30%, hypersensitivity to paromomycin and accumulation of halfmer ribosomes (19,24). It has been shown by *in vitro* poly(U)-dependent polyphenylalanine synthesis and puromycin reaction that deletion of eL24 results in alteration at the elongation step of translation (24,25). These observed phenotypes may reflect reduced ribosome functionality due to the absence of the whole eL24 protein or could have resulted from the impaired eB13 and/or B6 bridge formation.

Here, a detailed functional analysis of yeast eL24 is provided. The analysis indicates that mutations of the N-terminal residues (R43, R47) that contact with 18S rRNA and form conserved intersubunit B6 bridge, have no detectable effect on yeast cell viability and do not change the level of global translation. Deletion of the eB13 bridge forming region of eL24 compromises the formation of stable 80S ribosomes and affects the initiation and elongation of the ribosomes during *in vitro* translation. Remarkably, the N-terminal domain of eL24 plays a significant role at the initiation step of translation. These results suggest that the N-terminal region and the eB13 bridge forming region of eL24 execute distinctive functions during protein synthesis.

MATERIALS AND METHODS

Yeast strains and media

All *S. cerevisiae* strains used in this study were isogenic derivatives of S288C (26) and are listed in Supplementary Table S1.

Yeast cells were transformed using lithium acetate/single-stranded carrier DNA/polyethylene glycol method as described previously (27). Cells were grown in YPD (1% Bacto yeast extract, 2% Bacto peptone, 2% glucose) or synthetic complete medium (0.67% Bacto yeast nitrogen medium without amino acids, 2% glucose) supplemented with the appropriate amino acids and bases (28). For mass spectrometric analysis cells were grown in 'light' synthetic minimal medium (0.67% Bacto yeast nitrogen medium without amino acids, 2% glucose, 20 mg/l L-histidine, 20 mg/l uracil, 30 mg/l L-lysine, 20 mg/l L-arginine). To grow cells in 'heavy' synthetic minimal medium, L-lysine and L-arginine in the 'light' medium were exchanged to [$^{13}C_6/^{15}N_2$] L-lysine and [$^{13}C_6/^{15}N_4$] L-arginine. Agar (2%) was added to solid media. When required, the following concentrations of antibiotics were used: 300 μg/ml hygromycin B, 3 mg/ml neomycin, 0.5 mg/ml paromomycin or 1 mg/ml paromomycin.

Strains TYSC448 and TYSC455 were generated by one-step PCR based gene disruption (29) of the *RPL24A* and *RPL24B* genes, respectively. Deletion cassettes containing *hphMX6* (30) were PCR amplified and transformed into TYSC309 or TYSC310 strains. Strain TYSC488 was constructed by crossing TYSC448 and TYSC455. The resulting diploid was sporulated and tetrads were dissected.

Plasmids

All plasmids used in this study are listed in Supplementary Table S2. The *RPL24A* coding region with its 5′ upstream (973 bp) and 3′ downstream (461 bp) regions was amplified by PCR from genomic DNA and cloned between *PstI* and *XhoI* restriction sites into the *pRS314* vector, resulting plasmid *pRS314-RPL24*. To generate *pRS314-rpl24$_{1–111}$*, *pRS314-rpl24$_{1–80}$* and *pRS314-rpl24$_{1–65}$* plasmids, C-terminal coding regions for 44, 75 and 90 aa residues, respectively, were deleted by site-directed mutagenesis using overlap extension PCR. For construction of *pRS314-rpl24(R43A,R47A)* and *pRS314-rpl24$_{1–65}$(R43A,R47A)* plasmids, the site-directed mutagenesis was performed by overlap extension PCR to introduce R43A and R47A substitutions into *pRS314-RPL24* and *pRS314-rpl24$_{1–65}$*, respectively. To generate *pUC18-Fluc* and *pUC18-Rluc-Fluc* plasmids, *BamHI* restriction site between Renilla and Firefly luciferase genes in *pJD375* plasmid (31) was removed. After that, single Firefly luciferase gene and Renilla-Firefly fusion gene were amplified by PCR using primers encoding promoter region for T7 RNA-polymerase, 5′UTR of *PGK1* gene and poly(A)$_{30}$ sequence. Resulting *pT7/PGK1 5′UTR/Fluc/poly(A)$_{30}$* and *pT7/PGK1 5′UTR/Rluc-Fluc/poly(A)$_{30}$* fragments were

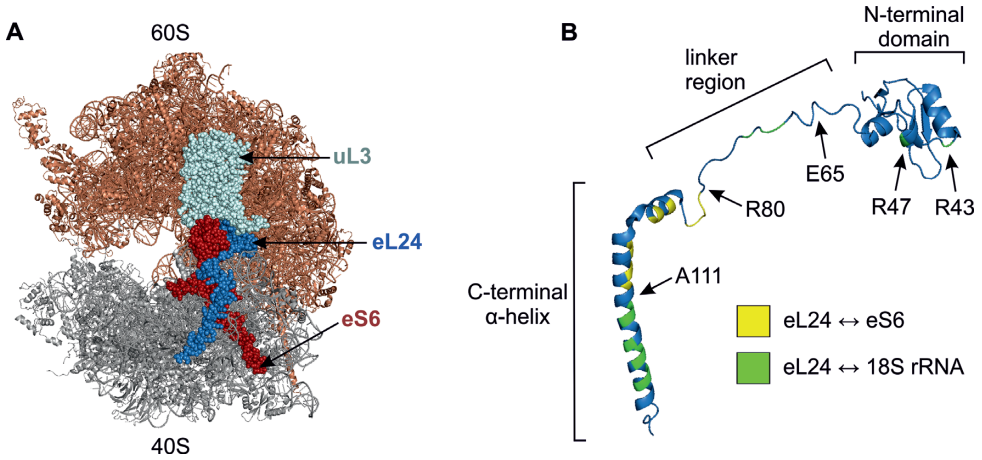

Figure 1. Eukaryotic eL24 protein. (**A**) *S. cerevisiae* 80S ribosome from P-stalk side. The 60S and 40S subunits, respectively, are shown in brown and grey. The proteins eL24 (blue), eS6 (red) and uL3 (light cyan) that form the eB13 and B6 bridges are shown. (**B**) Domain structure of eL24. Amino acid residues forming contacts with eS6 and 18S rRNA are colored yellow and green, respectively. R47 and R43 are B6 intersubunit bridge forming residues of eL24. E65 indicates the last amino acid of eB13Δ allele. This mutant mimics the archaeal version of eL24. R80 and A111 indicate the last amino acids of 81–155Δ and 112–155Δ alleles, respectively. Structures were generated by PyMol using coordinates from (11).

cloned between *BamHI* and *HindIII* restriction sites of the *pUC18* vector.

Temperature and antibiotic sensitivity assays

Yeast cells were grown in YPD medium at 30°C to OD_{600} = 0.8–1.0. Serially diluted cultures were spotted onto YPD plates and incubated at 16, 20, 25, 30 and 36°C for 2–5 days. To analyze sensitivity to aminoglycosides, cultures were serially diluted, spotted onto YPD plates supplemented with indicated concentrations of neomycin or paromomycin, and incubated at 25 and 30°C for 3–5 days.

Analysis of global level of translation

10 ml of yeast cell culture were grown in synthetic complete medium lacking tryptophan at 30°C to OD_{600} = 0.6–0.7. Mix of L-(U-14C) amino acids (CFB104, Amersham Inc., Bucks, England) was added to a final concentration of 0.00925 MBq/ml. One ml culture samples were taken every 15 min over 2 h of growth at 30°C. 100 μl of sample were used for optical density measurement, remaining 900 μl were precipitated by addition of 200 μl of 50% TCA. Samples were incubated 10 min on ice followed by 20 min at 70°C, and precipitates were collected onto Whatman GF/A filters (Whatman, Maidstone, England). Filters were washed three times with 5% TCA, three times with 70% ethanol and dried at 65°C for 10 min. Radioactivity was measured by scintillation counting. The dpm (disintegrations per minute) values divided by optical density values of the sample were plotted against the corresponding time points, slopes of obtained curves were calculated. The average and standard deviations for at least four biological replicates were calculated. Statistical significance was determined by the unpaired two sample Student's *t* test.

Ribosome–polysome profile analysis

Ribosome–polysome profile analysis was performed as described previously (16) with modifications. Namely, twenty A260 units of extract were layered onto 7–47% sucrose (w/w) gradient and centrifuged at 4°C in SW28 rotor (Beckman Coulter, Brea, CA, USA) at $\omega^2 t = 1.8 \times 10^{11}$. For 60S and 40S ratio quantification ribosome-polysome profile analysis was carried out with following modifications. The addition of cycloheximide to the cell cultures was omitted and Mg^{2+} was excluded from all buffers and sucrose gradients. Twenty A_{260} units of extract were layered onto 10–25% sucrose (w/w) gradient and centrifuged at 4°C in SW28 rotor (Beckman Coulter) at $\omega^2 t = 3.4 \times 10^{11}$. Areas under monosome (80S), polysome, 60S and 40S peaks were quantified by ImageJ and corresponding ratios were calculated. The average and standard deviations for at least three biological replicates were calculated. Statistical significance was determined by the unpaired two sample Student's *t* test.

In vitro reassociation of 80S

Assay for *in vitro* reassociation of 80S particles was performed as described previously (16), except that 5 mM of Mg^{2+} was used as a lower concentration for 80S reassociation.

Preparation of 80S ribosomes for mass spectrometric analysis

300 ml of yeast cells were grown in 'light' or 'heavy' synthetic minimal medium at 30°C to OD_{600} = 1.0–1.4. Cycloheximide was added to a final concentration of 100 μg/ml 15 min before harvesting. Cells were washed with 5 ml of ice-cold buffer A [30 mM HEPES–KOH (pH 7.5), 100 mM KCl, 10 mM $Mg(OAc)_2$, 2 mM DTT, 0.5 mM PMSF] supplemented with 100 μg/ml cycloheximide. After that, cells were disrupted with glass beads (Ø 0.25–0.5 mm) in Precellys 24 homogenizer (Bertin Technologies, Montigny-le-Bretonneux, France) (program: 6000 rpm, 3 × 60 s, pause 60 s). Obtained extracts were clarified for 3 × 5 min at 16 060 g. Thirty A_{260} units of extract were layered onto 7–47% sucrose gradient in buffer A and centrifuged at 4°C in SW28

rotor (Beckman Coulter) at $w^2t = 1.8 \times 10^{11}$. Gradients were monitored at $A_{260\,nm}$ and 80S fractions were collected. 80S ribosomes were pelleted by ultracentifugation in Ti50 rotor (Beckman Coulter) at $w^2t = 7.5 \times 10^{11}$. Obtained ribosomal pellet was dissolved in buffer A up to twenty A_{260} units per ml, aliquoted and stored at –80°C. Equal amount of 'heavy' ribosomes was mixed with 'light' ribosomes (0.5 A_{260} units) and precipitated overnight by 10% TCA. Mix was centrifuged for 45 min at 16 060 g. Ribosomal pellet was washed two times with 0.5 ml of 80% acetone, dried on air and stored at –20°C. Proteins were reduced, carbamidomethylated and digested as described previously (32), except carbamidomethylation was done by 5 mM chloroacetamide for one hour and mass spectrometry grade trypsin (Sigma-Aldrich, St. Louis, MO, USA) was used for digestion.

LC–MS/MS analysis

Two independent biological replicates were analysed as described previously (32) with modifications. Namely, peptides were analysed by LC-MS/MS with LTQ-Orbitrap XL (Thermo Scientific, Waltham, MA, USA). Peptides were eluted with 120 min 3–40% linear gradient of solvent B (80% acetonitrile, 0.5% acetic acid) in solvent A (0.5% acetic acid) at a flow rate of 250 nl/min.

Raw mass spectrometric data files were processed using MaxQuant software (version 1.5.6.0; (33) and searched against the *Saccharomyces* Genome Database protein sequences of all systematically named ORFs (http://www.yeastgenome.org; released 13 January 2015, accessed 22 November 2016) as described previously (32). Detection of at least two peptides was taken as minimal number to consider corresponding protein as detected. Peptides originated from protein eL41 were not detected in all biological replicates. Peptides originated from proteins eL39, eL40, P1A/B, P2A/B, uL10, uL11, uL14 and uL29 were excluded from analysis due to extremely high variability or absence in one of biological replicates. Obtained 'heavy'/'light' ratios for each ribosomal peptide were normalized against median 'heavy'/'light' ratio for all ribosomal peptides in each biological replicate. Following that, the average 'heavy'/'light' values over both replicates were calculated for each ribosomal protein using normalized peptide 'heavy'/'light' ratios. Fold changes in ratios of proteins in mutant ribosomes compared to control ribosomes were calculated. Statistical significance of changes in protein ratios was evaluated by unpaired two sample Student's t-test. Fold change higher or lower than 1.41 times ($\log_2 >= 0.5$ or $\log_2 <= -0.5$) and *P*-value lower than 0.05 ($-\log_{10} > 1.3$) were defined as statistically significant thresholds of difference.

Visualization and comparison of ribosome structures

UCSF Chimera 1.12 was used to visualize and compare structures of yeast and mammalian ribosomes with and without eIF5B and eIF6 factors (Protein Data Bank IDs 4V88 (11), 4V8Y (34), 4UJC (35), 4UJE (36) and 2X7N (37)).

Preparation of yeast cell-free extracts

Preparation of yeast cell-free extracts was performed as described previously (38,39) with modifications. Briefly, 1000 ml of yeast cells were grown in YPD at 30°C to OD_{600} = 2.0. Cells were harvested (10 min at 2404 × g), washed one time with 20 ml of ice-cold Mannitol Buffer A [30 mM HEPES–KOH (pH 7.5), 100 mM KOAc, 3 mM $Mg(OAc)_2$, 8.5% mannitol (w/v), 2 mM DTT] and three times with 10 ml Mannitol Buffer A. Cell pellet was weighed and 1.5 ml Mannitol Buffer A supplemented with 0.5 mM PMSF was added per gram of cells. Cells were disrupted with glass beads (Ø 0.25–0.5 mm) in Precellys 24 homogenizer (Bertin Technologies) (program: 6000 rpm, 3 × 60 s, pause 60 s). Extracts were clarified by centrifugation at 30 000 × g for 6 min, transferred to a new tubes and additionally clarified for 10 min. 2 ml of obtained extract was loaded onto 20 ml Sephadex G25 Fine column (Econo-Pac® Disposable Chromatography Column (Bio-Rad, Hercules, CA, USA)) and passed through the column at a flow rate ∼0.5 ml/min in Buffer A [30 mM HEPES–KOH pH 7.5, 100 mM KOAc, 3 mM $Mg(OAc)_2$, 2 mM DTT, 0.5 mM PMSF]. 200 μl fractions were collected, and fractions with A_{260} higher than 75% of the maximal A_{260} were pooled. $CaCl_2$ was added to the obtained extract to a final concentration of 0.5 mM followed by addition of micrococcal nuclease (Thermo Scientific) to a final concentration of 0.18 U/μl. Extract was incubated for 10 min at 25°C. EGTA (pH 8.0) was added to the extract to a final concentration of 0.2 mM. The nuclease treated extract was aliquoted and stored at –80°C.

mRNA synthesis

pUC18-Fluc and *pUC18-Rluc-Fluc* plasmids were linearized at *BamHI* restriction site and used as a template for *in vitro* transcription reaction. To synthesize mRNA *in vitro*, 50 μl transcription mixture [1 μg linear DNA, 3.75 mM of each rNTP, 50 mM NH_4Cl, 200 mM HEPES–KOH (pH 7.5), 30 mM $MgCl_2$, 30 mM DTT, 2 mM spermidine, 40 U RiboLock RI (Thermo Scientific), 250 U home-made T7 RNA-polymerase] was incubated for 2 h at 42°C. 10 U of DNaseI (VWR Life Science AMRESCO, Radnor, PA, USA) was added to the mixture followed by incubation for 20 min at 37°C. mRNA was purified by acidic phenol-chloroform extraction, precipitated by ethanol, aliquoted and stored at –80°C. mRNA capping was performed using Vaccinia Capping System (New England Biolabs, Ipswich, MA, USA) in accordance with the manual. Capped mRNA was purified with RNeasy® Mini Kit (QUIAGEN GmbH, Hilden, Germany) according to the manual, aliquoted and stored at –80°C. The same batch of mRNA was used for parallel analysis of all cell-free extracts.

In vitro translation reaction

To determine luciferase activity time course and time of the first appearance of the luminescence signal, 15 μl of 2× translation mixture [44 mM HEPES–KOH (pH 7.5), 240 mM KOAc, 4 mM $Mg(OAc)_2$, 1.5 mM ATP, 0.2 mM GTP, 3.4 mM DTT, amino acid mix (0.08 mM of each), 50 mM creatine phosphate, 500 ng mRNA, 0.4 μg/μl creatine phosphokinase (Sigma-Aldrich), 60 U RiboLock RI

(Thermo Scientific)] and 15 μl of yeast nuclease treated extract were preincubated for 5 min at 25°C. After that, yeast extract was added to the translation mixture (50% of final volume) and incubated at 25°C.

At time-points indicated 2 μl reaction samples were frozen in liquid N_2. Reaction samples were thawed on ice immediately before luciferase activity measurement. In case of single luciferase reporter, Firefly luciferase activity was measured by Steady-Glo® Luciferase Assay System (Promega, Madison, WI, USA). In case of dual luciferase reporter, Firefly and Renilla luciferase activities were measured by Dual-Luciferase® Reporter Assay System (Promega). All measurements were done using Tecan Infinite M200 Pro plate reader (Tecan Group Ltd., Männedorf, Switzerland). For each strain at least three independent extracts were analyzed, each extract was analyzed by at least two independent reactions.

To determine slope of the luciferase activity time course, gcFit function in 'grofit' package for R was used. To determine processivity of ribosomes, the slope value of the Firefly luciferase activity time course was divided by the slope value of the Renilla luciferase activity time course. Statistical significance was determined by the unpaired two sample Student's *t* test.

RESULTS

Protein eL24 and intersubunit bridge eB13 are important for the optimal cell growth

Ribosomal protein eL24 is present in both eukaryotic and archaeal ribosomes, but there is no bacterial homolog of eL24. Eukaryotic eL24 is composed of an N-terminal domain, a linker region and a C-terminal α-helix, while archaeal homolog consists of only N-terminal domain (20). Yeast eL24 is one out of three ribosomal proteins that participates in formation of two distinct intersubunit bridges, eB13 and B6 (Figure 1B and Supplementary Figure S1) (11). The C-terminal α-helix and linker region of eL24 form contacts with 40S protein eS6 and 18S rRNA helices 6, 10 and 44, yielding the main part of the eukaryote-specific eB13 bridge. Arginine residues at positions 43 and 47 in the N-terminal globular domain of eL24 interact with 18S rRNA helix 44 and give rise to the conserved B6 bridge. To dissect functions of these two bridges, several eL24 mutant strains were constructed (Table 2). In budding yeast genome, eL24 is encoded by the pair of paralogous genes *RPL24A* and *RPL24B*. In mutant eL24Δ, both paralogous genes were deleted (*rpl24AΔrpl24BΔ*). In eL24 control cells, the full-length eL24A (155 aa residues) was expressed in *rpl24AΔrpl24BΔ* background. In mutant B6Δ, the full-length eL24 harboring R43A and R47A substitution in its N-terminal domain was expressed. This mutant was deficient in B6 bridge formation. To analyze the importance of the eB13 bridge only, three eB13 bridge mutants were constructed. In mutant 112–155Δ, the N-terminal 111 aa residues of eL24 were expressed. This eL24 variant has lost the contacts with h6 and h10. In mutant 81–155Δ, the N-terminal 80 aa residues of eL24 were expressed. This eL24 variant retained interaction only with h44. In mutant eB13Δ, the 65 aa residues long eL24 was expressed. This variant of eL24 mimicked the archaeal version of eL24 and had no contacts with eS6, h6, h10 and h44. In double bridge mutant eB13ΔB6Δ, the 65 aa residues long eL24 harboring R43A and R47A substitutions was expressed in cells lacking eL24.

Table 1. Components of B6 and eB13 bridges in the post-translocational state of the *S. cerevisiae* ribosome from (11)

Bridge	60S component	40S component		
B6	eL24	R43	h44	G1670
		R47		U1724
eB13	uL3	S297	eS6	H22
		F298		R25
	eL24	K70	h44	A1714
		R71		G1713
		R73		A1712
		P81	eS6	P130
		I82		F144
		T83		R132
		G84		R159
		I90		F144
		R93		F145
		R93		F156
		R94		F144
		R101		D151
		R105		E150
		K108		D155
		D112	h10	U280
		K113		U280
		K117		U278
		K120		G274
		R123		G273
		K124		G274
		D119	h6	U75

Serial dilutions spot-test was performed on rich medium at different temperatures in order to examine the growth characteristics of the constructed eL24 mutants (Figure 2A). Mutants B6Δ and 112–155Δ exhibited wild-type growth at all analyzed temperatures. Mutants 81–155Δ, eB13Δ and eB13ΔB6Δ also demonstrated wild-type growth at 25–36°C, but cold sensitivity at 16°C. Deletion of the whole eL24 provoked the most substantial effect on yeast cells manifested in slow growth phenotype at 25–36°C. The cold sensitivity phenotype was obvious already at 20°C. To determine the impact of constructed eL24 mutations on yeast growth in more detail, generation times of eL24 mutants were measured in rich medium at 30°C (Table 2). Mutants B6Δ and 112–155Δ displayed growth rate similar to control, while mutants 81–155Δ, eB13Δ and eB13ΔB6Δ exhibited prolongation of generation times. Loss of the eL24 reduced growth rate by ∼30%, which is consistent with previously published data (19,24).

Global levels of translation was evaluated for more extensive characterization of eL24 mutants (Figure 2B). The incorporation of radioactive isotope labeled amino acids in newly synthesized proteins in exponentially growing yeast cells was determined. No significant change in the global levels of translation was observed in case of B6Δ and 112–155Δ mutants. The levels of translation were reduced by

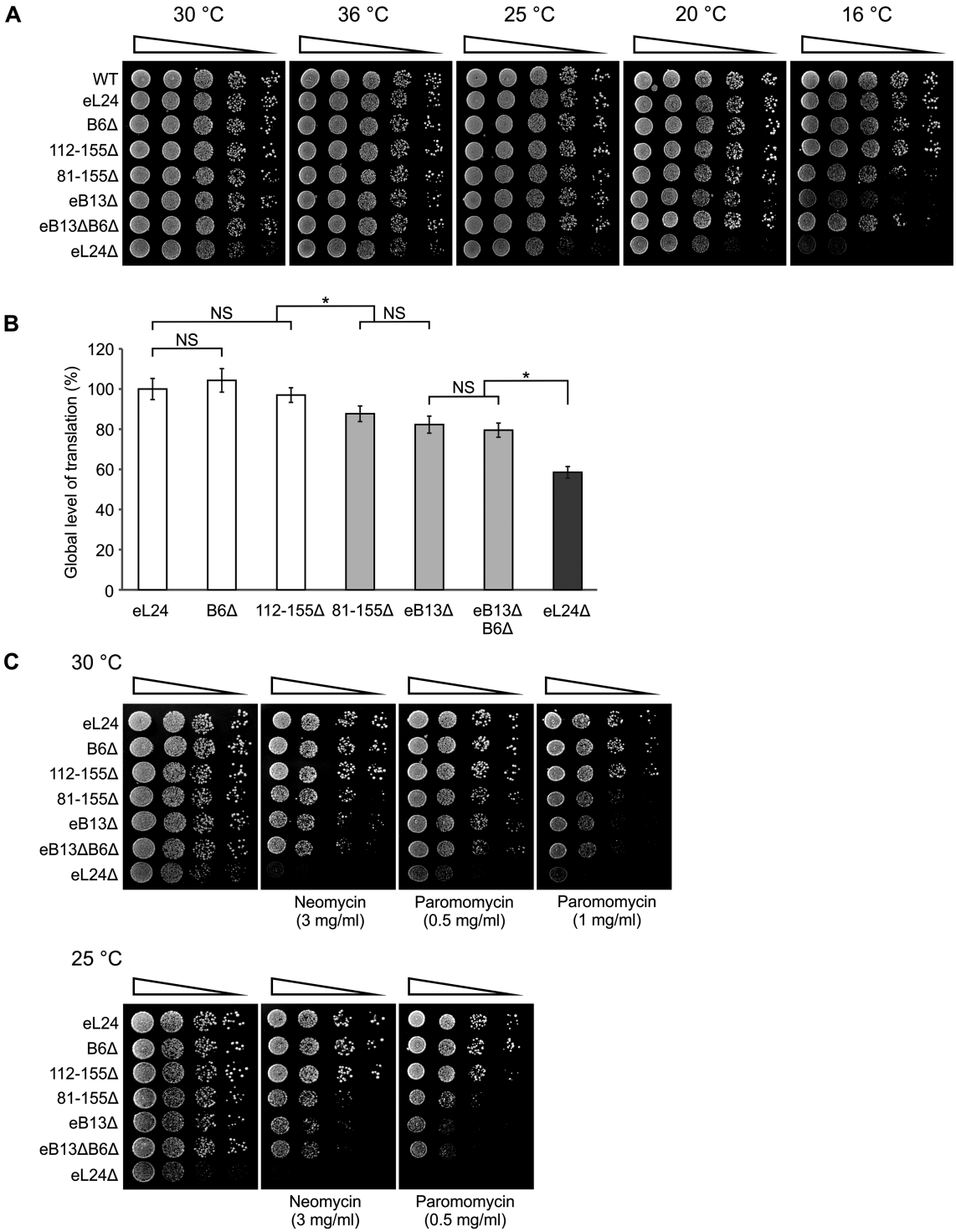

Figure 2. Phenotypic characterization of eL24 mutants.Growth phenotypes (**A**) and aminoglycoside sensitivity (**C**) of eL24 mutants. Serial dilutions of wild-type (WT, TYSC309), *rpl24AΔrpl24BΔ* strain (eL24Δ, TYSC488) and *rpl24AΔrpl24BΔ* strains carrying either eL24 wild-type (eL24) or mutant alleles (B6Δ, 112–155Δ, 81–155Δ, eB13Δ or eB13ΔB6Δ) were spotted onto rich medium without or with indicated antibiotics. The cells were grown at the indicated temperatures for 2–5 days. (**B**) Analysis of global level of translation of *rpl24AΔrpl24BΔ* strains carrying either eL24 wild-type (eL24) or mutant (B6Δ, 112–155Δ, 81–155Δ, eB13Δ or eB13ΔB6Δ) alleles and *rpl24AΔrpl24BΔ* strain (eL24Δ, TYSC488). Radioactive isotope labeled amino acids mix was added to exponentially growing cells in synthetic complete medium lacking tryptophan at 30°C. Culture samples were taken at every 15 min over 2 h of incubation. Samples were TCA precipitated and incorporation of radioactive label over time was measured. Obtained values of disintegrations per minute (DPM) were plotted and slope was calculated. The average (mean ± SD) slope values from at least four biological replicates are plotted. Statistical significance was determined by the unpaired two sample Student's *t* test (*$P < 0.01$; NS, not significant).

Table 2. Analyzed eL24 mutants

Strain name	Abbreviation	Length of eL24 (aa)	Deleted contacts/regions	Substitutions	Generation time (min)[a]
eL24	eL24	155	-	-	86.5 ± 3.2
$eL24_{R43A, R47A}$	B6Δ	155	-	R43A, R47A	87.5 ± 2.0
$eL24_{1–111}$	112–155Δ	111	h10, h6		86.1 ± 2.0
$eL24_{1–80}$	81–155Δ	80	eS6, h10, h6		99.5 ± 1.4[b]
$eL24_{1–65}$	eB13Δ	65	α-helix, linker	-	99.1 ± 3.7[b]
$eL24_{1–65, R43A, R47A}$	eB13ΔB6Δ	65	α-helix, linker	R43A, R47A	98.7 ± 3.3[b]
eL24Δ	eL24Δ	-	whole eL24	-	111.0 ± 3.9[c]

[a]Generation times were calculated from at least four independent experiments in triplicate, means are shown with standard deviations
[b]Indicates a statistically significant difference from eL24 and eL24Δ strains ($P < 0.01$; unpaired two sample Student's t test)
[c]Indicates a statistically significant difference from all other analyzed strains ($P < 0.01$; unpaired two sample Student's t test)

15–20% in 81–155Δ, eB13Δ and eB13ΔB6Δ mutants compared to eL24 control cells. Loss of the L24 reduced the global translation by >40%.

It has been previously shown that yeast cells lacking eL24 protein are more sensitive to paromomycin than wild-type cells (24). Aminoglycoside antibiotics, such as paromomycin and neomycin, are known to induce missense errors during protein synthesis (40). Therefore, growth defects in the presence of these antibiotics indicate reduced functionality of ribosomes. Serial dilutions spot-test was used in this study to more extensively analyze the effect of aminoglycosides on cells growth on rich medium at 25°C and 30°C (Figure 2C). Mutants B6Δ and 112–155Δ exhibited wild-type growth in the presence of either paromomycin or neomycin at both analyzed temperatures. Mutants 81–155Δ, eB13Δ and eB13ΔB6Δ conferred remarkable hypersensitivity to both of the analyzed aminoglycosides. Mutant lacking eL24 is even more sensitive to the drugs than the bridge mutants, being inviable in the presence of 1 mg/ml paromomycin at 30°C and neomycin or paromomycin at 25°C (Figure 2C).

Protein synthesis in yeast cells growing on rich medium has been shown to be limited by the availability of functional ribosomes (41). In the light of this knowledge, analyzed mutants can be divided into three phenotypic groups. First group is formed by mutants B6Δ and 112–155Δ that exhibited wild-type phenotype in all assays used. These data show that neither B6 bridge nor region of eL24 contacting with h6 and h10 does not play a significant role in the ribosome functioning. For that reason, mutants B6Δ and 112–155Δ were not included in the further analysis. Second group consists of mutants 81–155Δ, eB13Δ and eB13ΔB6Δ. These mutants displayed reduced ribosome functionality, as can be deduced from cold sensitivity, hypersensitivity to aminoglycosides and decreased global levels of translation. More importantly, similarity of phenotypes exhibited by 81–155Δ and eB13Δ mutants points at the interaction between eL24 and eS6 as a key component of the eB13 bridge. The eB13Δ mutant was chosen for further analysis as a representative of eB13 bridge functions. Third group consists of eL24Δ mutant. Interestingly, lack of eL24 leaded to intensified cold sensitivity and hypersensitivity to aminoglycosides along with lower general level of translation if compare to the second group of mutants. This indicates that the N-terminal domain of eL24 may execute additional function(s).

eB13 bridge is important for the integrity of protein synthesis

Previous studies have shown that absence of eL24 causes accumulation of stalled preinitiation complexes that have been referred to as halfmers (19,24). Appearance of halfmers can be caused by either compromised eB13 bridge or absence of the whole eL24 protein. To test this, eL24 control, eB13Δ and eL24Δ mutant cells grown in rich medium at 30°C or 20°C were subjected to ribosome–polysome profile analysis by sucrose gradient sedimentation (Figure 3A). eL24 control cells showed high amount of polysomes (polysome/monosome ratio ∼2.7) and low amount of free 40S and 60S subunits at both analyzed temperatures (Figure 3A, B). Defectiveness of eB13 or lack of eL24, in turn, provoked reduced level of polysomal fraction by ∼36% at 30°C and by ∼45% at 20°C (Figure 3A, B), which is consistent with measured global levels of translation (Figure 2B). In addition, both mutants exhibited accumulation of free subunits and halfmers at 20°C (Figure 3A). This data indicates that appearance of halfmers is specific for cells with compromised eB13 bridge.

Halfmers may be caused by limited amount of functional 60S subunits in mutant extracts as a consequence of defective eB13 bridge. Ribosome-polysome profiles did not reveal extra peaks or changed sedimentation values of 60S subunits or ribosomal particles (Figure 3A). In view of this, HPLC-MS/MS approach was used for a more extensive analysis of composition of mutant 80S ribosomes. 'Light' mutant 80S ribosomes and 'heavy' wild-type 80S ribosomes obtained via stable isotope labeling by amino acids in cell culture (SILAC) were isolated by separation in sucrose density gradients, mixed together at an equimolar ratio and 'heavy'/'light' ratios of proteins were determined by MS/MS. No significant changes in the stoichiometry of ribosomal proteins were detected in 80S ribosomes of eB13Δ or eL24Δ mutants if compared to eL24 control (Figure 4A, B). Presence of eL24 protein in mutant ribosomes was analyzed in more detail. In ribosomes lacking eL24 protein no peptides corresponding to eL24 were detected. In ribosomes compromised in eB13 bridge formation, peptides originated only from N-terminal domain of eL24 were observed (Supplementary Figure S2). To compare stoichiometry of eL24 protein in ribosomes of eB13Δ mutant and control cells, 'heavy/light' ratios of those peptides that correspond to the N-terminal domain of eL24 were calculated. Analysis of 5 unique peptides indicated that these peptides were present in eB13Δ mutant and con-

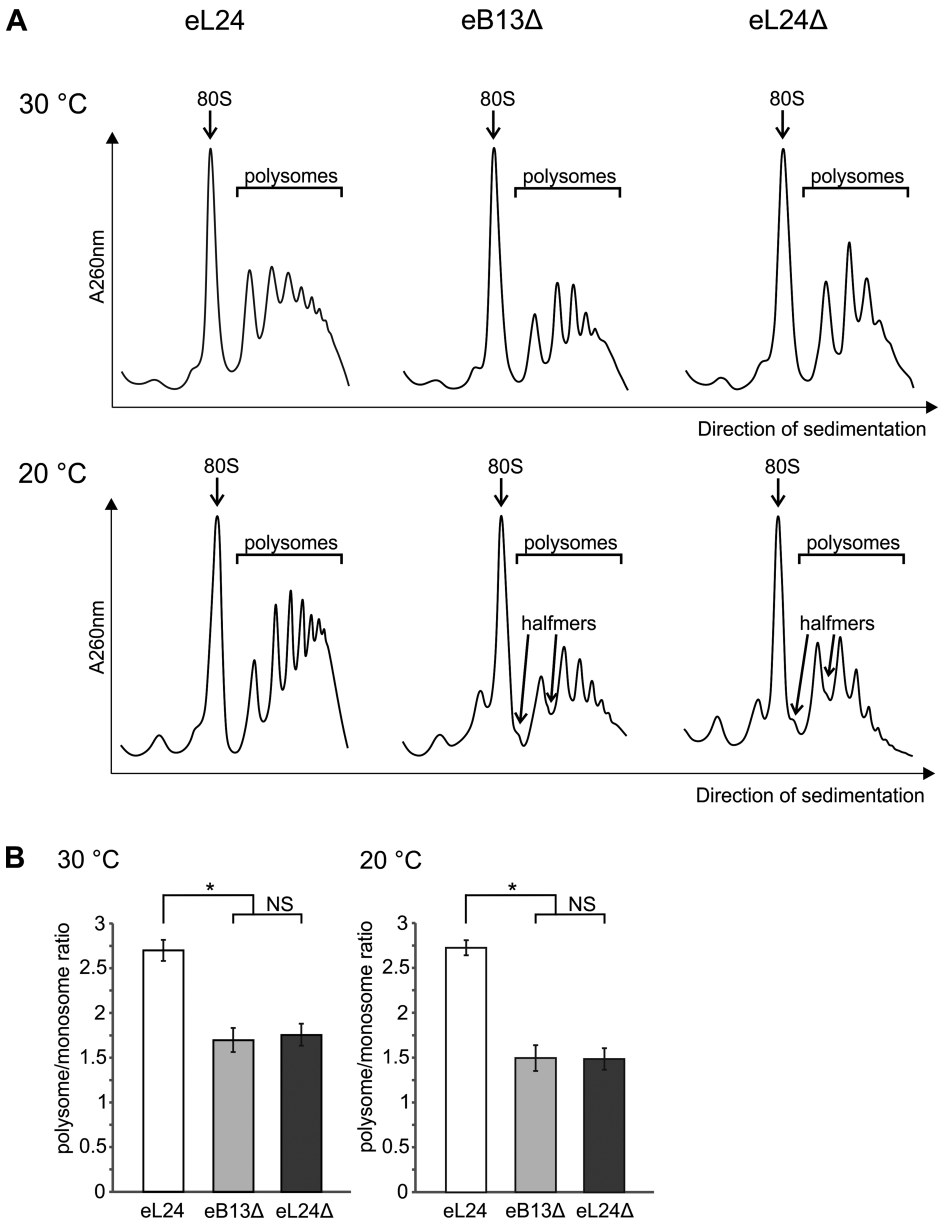

Figure 3. The eB13 bridge controls the integrity of polysomes. (**A**) Analysis of ribosome-polysome profiles of *rpl24AΔrpl24BΔ* strains carrying either eL24 wild-type (eL24) or mutant (eB13Δ) allele and *rpl24AΔrpl24BΔ* strain (eL24Δ, TYSC488) by sedimentation in sucrose density gradient. Strains were grown in rich medium at 30°C or 20°C to mid-exponential phase. The whole cell extracts were prepared in presence of cycloheximide and high concentration of Mg^{2+} and subjected to sedimentation analysis in 7%- 47% sucrose gradients. Gradients were visualized at 260 nm (A260 nm). Sedimentation is from left to right. The peaks of monosomes (80S), polysomes and halfmers are indicated. (**B**) Polysome/monosome ratios of extracts analyzed in (A). Areas under monosome (80S) and polysome peaks from (A) were quantified by ImageJ and polysome/monosome ratios were calculated. The average (mean ± SD) ratios of at least three biological replicates are plotted. Statistical significance was determined by the unpaired two sample Student's *t* test (*$P < 0.01$; NS, not significant).

trol ribosomes in similar molar ratio (Supplementary Figure S2). Altogether, analysis of detected ribosomal proteins indicates that ribosomes compromised in eB13Δ formation or lacking eL24 have similar to control ribosomes composition and stoichiometry of proteins. In addition, truncated version of eL24 is effectively incorporated into 60S subunits of eB13Δ mutant.

Appearance of halfmers in extracts of eB13Δ mutant may also be due to decreased level of 60S subunits. To measure relative amounts of available 60S and 40S subunits more precisely, extracts of eL24 control, eL24Δ and eB13Δ mutant cells were resolved in sucrose gradients at low concentration of Mg^{2+} (Supplementary Figure S3A). Compared to eL24 cells, mutants with compromised eB13 bridge or without eL24 exhibited reduction in amount of 60S subunits at both analyzed temperatures (Supplementary Figure S3B). Furthermore, eL24Δ mutant cells have lower level of 60S subunits than eB13Δ cells (Supplementary Figure S3B). This data demonstrates that appearance of halfmers is indeed caused by decreased amount of 60S subunits. It is

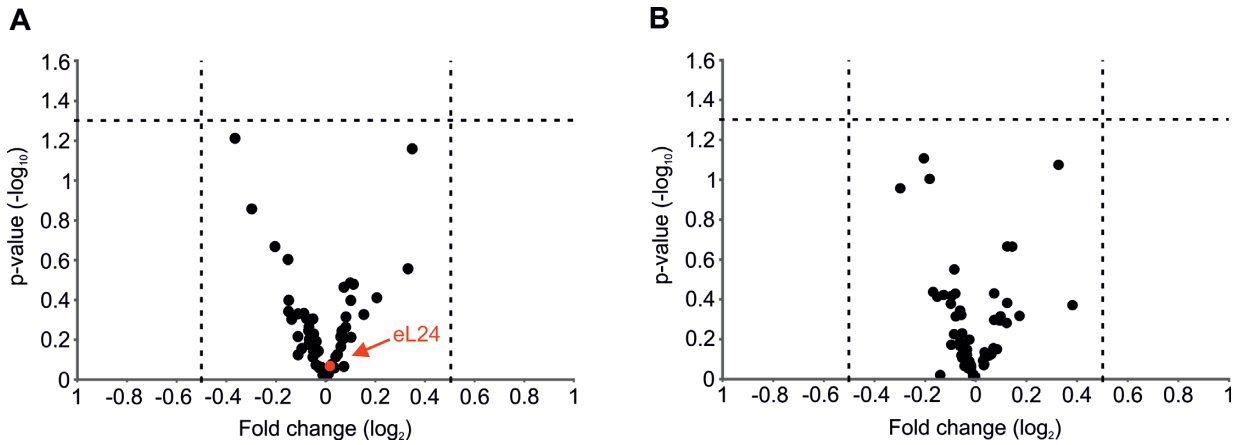

Figure 4. Mass spectrometric analysis of ribosomes from eL24 mutants.Volcano plots of changes in stoichiometry of ribosomal proteins in ribosomes of eB13Δ mutant *versus* ribosomes from control strain (**A**) and ribosomes of eL24Δ mutant *versus* ribosomes from control strain (**B**). Horizontal dashed line indicates threshold *P*-value of 0.05 ($-\log_{10} = 1.3$). Vertical dashed lines indicate threshold fold change values 1.41 ($\log_2 = 0.5$) and –1.41 ($\log_2 = -0.5$). Red circle indicates position of eL24 protein.

possible that depletion or even truncation of eL24 leads to defects in the assembly of 60S subunits and consequently to the decrease in their level. These defects can be accompanied by imbalance in stoichiometry of biogenesis factors. It is known that the incorporation of eL24 into 60S subunit at the cytoplasmic step of maturation is preceded by the removal of Rlp24 by AAA-ATPase Drg1 (21,23). Cytoplasmic step also involves binding/release of other biogenesis factors: Nog1, Rei1, Arx1, Sdo1, Yvh1, Mtr4, Efl1, Tif6 and (21,22,42–46). Mass spectrometric analysis showed that biogenesis factors are not present in the ribosomes from eL24, eB13Δ and eL24Δ strains. This suggests that ribosome maturation occurs similarly in all analyzed strains. Therefore, the cause of the reduction of 60S subunits remains unknown.

Altogether, analysis of mutant cells having ribosomes with compromised eB13 bridge revealed diminished levels of polysomes at both temperatures and presence of halfmers in ribosome–polysome profiles at 20°C. This indicates that the reduced level of translation in eB13Δ mutant cells (Figure 2B) may be caused by the alterations at the initiation step of translation.

eB13 bridge contributes to the stable subunit joining *in vitro*

To study the contribution of eB13 bridge to subunit joining independently of additional trans-acting factors, *in vitro* reassociation activity of salt-washed ribosomal subunits from eL24 control cells, eB13Δ and eL24Δ mutant cells was determined (Figure 5). Two A_{260} units of control 40S subunits was mixed with two A_{260} units of control or mutant 60S subunits at different Mg^{2+} concentrations, and formation of 80S was analyzed by sucrose gradient sedimentation. Control 40S and 60S subunits reassociated already at 5 mM Mg^{2+} concentration. In contrast, 60S subunits of both mutants were deficient in 80S ribosome formation at 5 mM Mg^{2+} and started to form intermediate particles at 10 mM Mg^{2+} in case of compromised eB13 bridge and at 15 mM Mg^{2+} in case of lack of eL24 protein. Intermediate particles migrate in sucrose gradient between 60S and 80S subunits peaks, possibly due to loose interactions of mutant 60S with 40S subunits. All analyzed 60S subunits reassociated completely in the presence of saturating amounts of deacylated tRNA at 20 mM Mg^{2+} demonstrating that 60S subunits of mutant strains are able to form 80S ribosomes. This data points that trans-acting factors can compensate the loss of the intersubunit bridge, which is consistent with previous study (16). Overall, analysis of *in vitro* subunit joining indicates that the eB13 bridge region of eL24 is important for the correct 80S ribosome formation. This may represent involvement of the eB13 bridge in the translation initiation process.

eL24 is important for the efficient *in vitro* translation

The above findings indicate that the N-terminal domain and the eB13 bridge forming region of eL24 are important for the optimal cell growth (Figure 2A, B, Table 2). Bridge eB13 is also important for the stable intersubunit joining *in vivo* and *in vitro* (Figures 3A and 5). In order to understand these effects in the light of translation dynamics, cap- and polyA tail-dependent translation of mRNA encoding a single Firefly luciferase was examined in cell-free translation extracts (Figure 6A). As a first approach, the time course of *in vitro* translation over 80 min was monitored (Figure 6B). Reaction samples were taken at different time points from the reaction mix and subjected to the luciferase activity measurement. The maximum rate of translation was determined from the slope of the linear part of the obtained luciferase activity time course (Figure 6A-C). Compared to control extract, the rate of translation was reduced ∼1.6-fold in case of compromised eB13 bridge and ∼9.9-fold in case of lack of eL24 (Figure 6C). These data demonstrate that both eB13 bridge forming region and N-terminal domain of eL24 are required for the efficient *in vitro* translation. Considering that initiation has been shown to be the rate limiting step of translation, reduced slope of the luciferase activity represents decreased rate of initiation in extracts of both mutants (41,47–49).

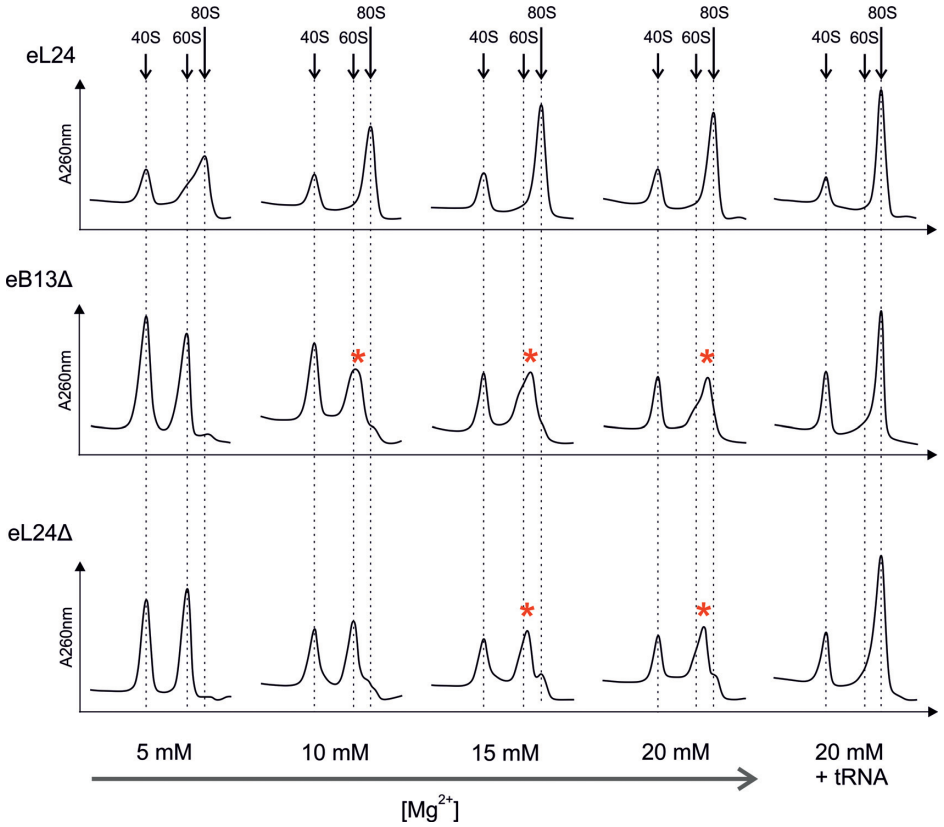

Figure 5. The eB13 bridge contributes to the stable ribosome subunit joining *in vitro*. Salt-washed 60S and 40S subunits were purified from *rpl24AΔrpl24BΔ* cells carrying either eL24 wild-type (eL24) or mutant (eB13Δ) allele and *rpl24AΔrpl24BΔ* cells (eL24Δ, TYSC488) grown in rich medium at 30°C to mid-exponential phase. Two A260 units of wild-type 40S subunits were mixed with two A260 units of 60S containing wild-type or mutant eL24 and incubated in the presence of indicated Mg^{2+} concentration for 20 min at 30°C. Reactions were also performed in the presence of 20 mM Mg^{2+} and saturating concentration of deacylated tRNA (20 mM + tRNA). Formation of 80S particles was analyzed in 10–30% sucrose gradients in the presence of appropriate Mg^{2+} concentrations. Sedimentation is from left to right. The peaks of free 40S, 60S and monosomes (80S) are indicated by arrows, the intermediate particles are highlighted with asterisks.

To measure how long it takes for the ribosome to complete the translation of single Firefly luciferase molecule, time of the first appearance (TFA) of the luminescence signal was measured in cell-free translation extracts from eL24 control, eB13Δ and eL24Δ cells (Figure 6A and 6D). TFA represents time required for one round of translation and contains time needed for initiation, elongation and termination, but not ribosome recycling. Folding of Firefly luciferase has been previously shown to occur co-translationally (50). Therefore, enzyme is active immediately when released form the ribosome and TFA is not affected by protein folding (50). The TFA value for control extract was 2.42 ± 0.58 min. Ribosomes with compromised eB13 bridge or lacking eL24 had respectively 1.8 and 3.1 times longer TFAs than control extract (Figure 6D). Prolonged TFAs indicate that mutant ribosomes need more time to complete translation of the luciferase molecules as compared to control ribosomes.

TFA values may also be affected by limited processivity of ribosomes during translation elongation (51,52). To determine processivity of ribosomes, synthesis of a fusion Renilla-Firefly luciferase over 80 minutes in cell-free translation extracts was examined (Supplementary Figure S4A-C), and slopes of the linear parts of the obtained Renilla and Firefly luciferase activity time courses were determined. Slope of the Renilla luciferase activity time course represents number of ribosomes that completed synthesis of Renilla luciferase only. In turn, slope of the Firefly luciferase activity curve depends on the number of ribosomes that completed synthesis of a whole fusion Renilla-Firefly luciferase. Therefore, ratio between slopes of Firefly and Renilla luciferase activity time courses reflects processivity of ribosomes. Compared to control, extracts of both mutant displayed similar slope ratios (Supplementary Figure S4D), showing that the loss of eB13 bridge or complete eL24 does not cause the significant changes in processivity.

To assess elongation rate of ribosomes with compromised eB13 bridge or without eL24, difference between TFA values of Firefly and Renilla luciferase signal was measured (Figure 7). The time required for ribosomes to synthesize Firefly luciferase after completion of Renilla luciferase synthesis depends on the elongation rate of ribosomes. Ribosomes in control extracts needed 5.16 ± 0.16 min to complete synthesis of fusion luciferase protein, while for ribosomes of both mutants this time was similarly extended by ∼1.3 times (Figure 7). Prolonged time difference between

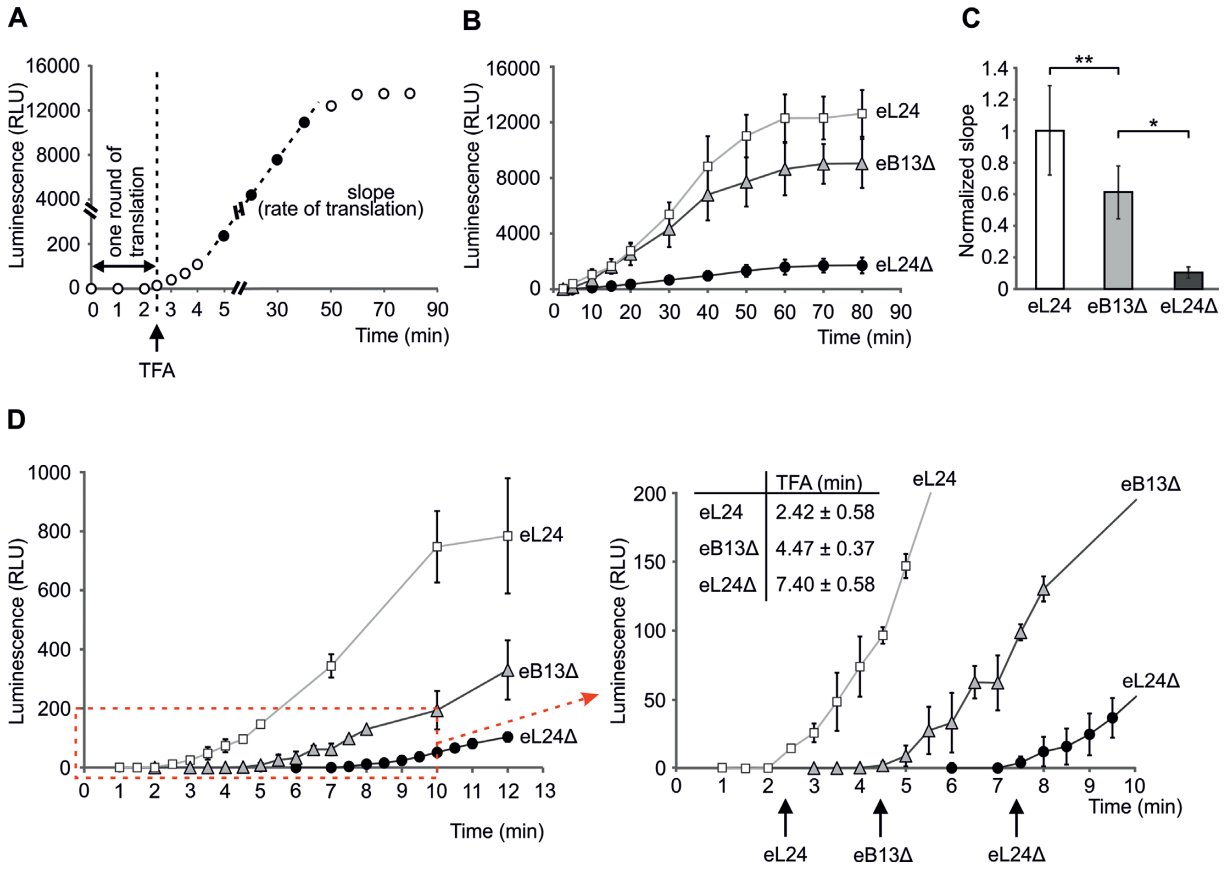

Figure 6. The eL24 is important for the efficient *in vitro* translation. (**A**) Schematic representation of a single Firefly luciferase activity curve obtained by *in vitro* translation analysis. Time of the first appearance (TFA) of the luminescence signal reflects the time needed for one round of translation and combines times of initiation, elongation and termination. Slope of linear part of luciferase activity curve reflects the rate of *in vitro* translation. (**B**) Synthesis of a single Firefly luciferase in yeast extracts prepared from *rpl24AΔrpl24BΔ* cells carrying either eL24 wild-type (eL24) or mutant (eB13Δ) allele and *rpl24AΔrpl24BΔ* cells (eL24Δ, TYSC488). *In vitro* translation was carried out at 25°C in 30 μl starting volume using 500 ng of mRNA as a template. For each strain at least three independent extracts were analyzed, each extract was analyzed by at least two independent reactions. The average (mean ± SD) relative light units (RLU) of all replicates are plotted. (**C**) Normalized slopes of linear parts of luciferase activity curves from (B). The average (mean ± SD) slopes of all replicates are plotted. Statistical significance was determined by the unpaired two sample Student's t test (**$P < 0.05$; *$P < 0.01$). (**D**) Time of the first appearance of the luminescence signal (TFA) in extracts from (B). *In vitro* translation was carried out at 25°C in 30 μl starting volume using 500 ng of mRNA as a template. For each strain at least two independent extracts were analyzed, each extract was analyzed by at least two independent reactions. The average (mean ± SD) relative light units (RLU) of all reactions are plotted. Red dashed-line square marks the area that was magnified and displayed on the right. TFAs are indicated by arrows. The average (mean ± SD) TFA values of all reactions are presented above the plot.

TFA values reflects similarly decreased elongation rates of mutant ribosomes.

Overall, extracts of eB13Δ mutant demonstrated altered rate of both initiation (Figure 6C) and elongation (Figure 7B) steps of translation if compared to control extracts. Therefore, ∼1.8 slower synthesis of single Firefly luciferase molecule in this mutant (Figure 6D) is caused by the combination of decreased initiation and elongation rates of ribosomes with compromised eB13 bridge. Rates of elongation of eB13Δ and eL24Δ mutant ribosomes did not differ against each other since ribosomes of both mutants required similar time to complete synthesis of fusion Renilla-Firefly luciferase protein (Figure 7B, C). This indicates that eB13 bridge has an important function during elongation step of translation. In turn, extracts of eL24Δ showed lower rate of initiation if compared to eB13Δ extracts (Figure 6C), suggesting that the N-terminal domain of eL24 has additional role during translation.

DISCUSSION

The eukaryotic ribosomal protein eL24 is composed of three domains: N-terminal domain, linker region and C-terminal α-helical domain (11) (Figure 1B). In this study, the functional importance of different domains of eL24 was investigated.

The C-terminal α-helical domain and the linker region of eL24 form the eB13 bridge through the interactions with eS6, h6, h10 and h44 (Figure 1B, Supplementary Figure S1). Phenotypic analysis of several eB13 bridge mutants revealed that functionality of this bridge primarily depends on the protein–protein type contacts between eL24 (aa residues 81–108) and eS6 (aa residues 130–155) (Figure 2A–C). Protein eS6 is known to undergo phosphorylation (S232 and S233 in yeast) in response to variety of stimuli, but the physiological role of phosphorylation is yet not known (53). This study revealed another important function of eS6, which is the formation of the eB13 bridge.

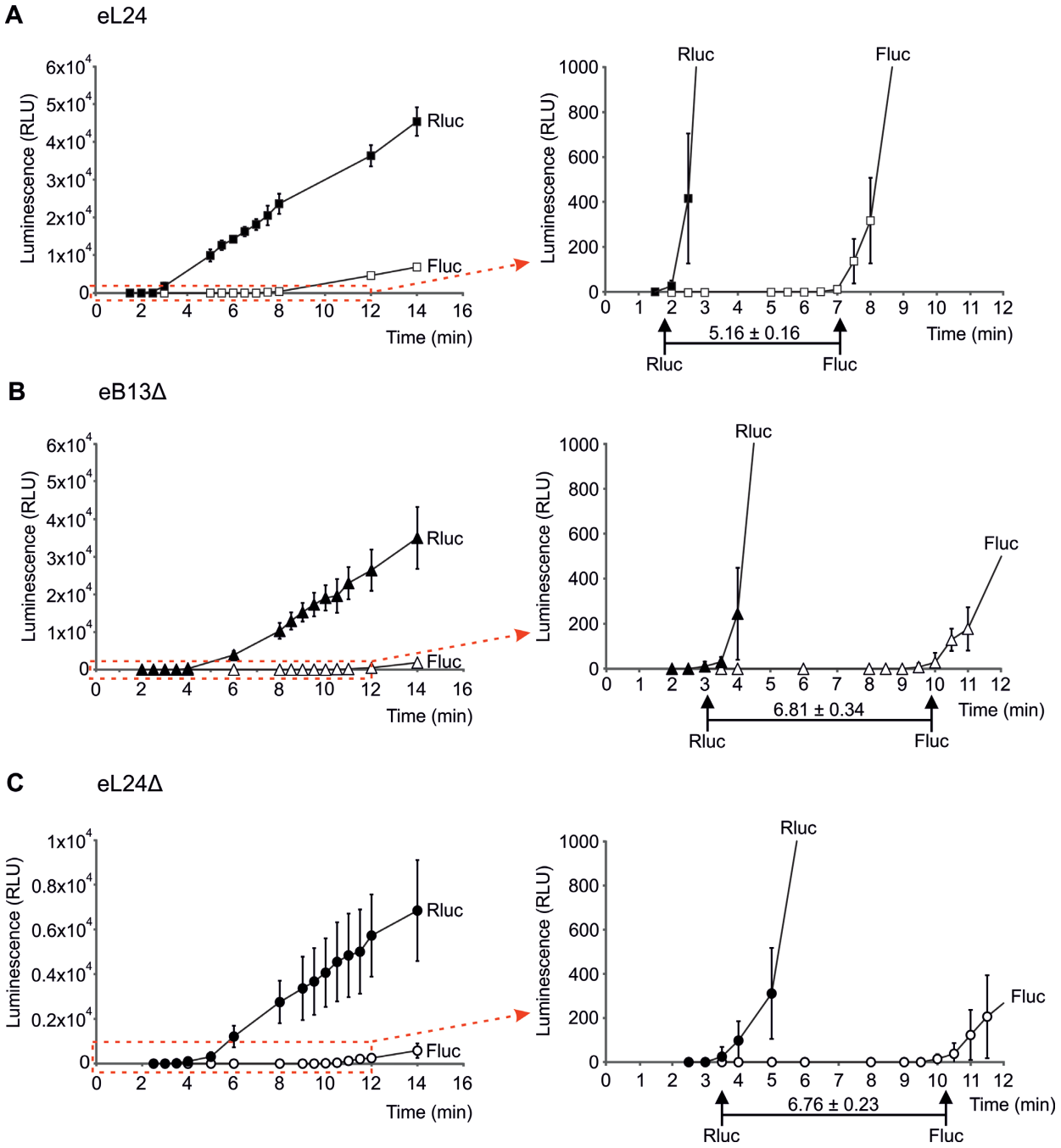

Figure 7. The eB13 bridge is important for the elongation step of *in vitro* translation.Synthesis of fusion Renilla-Firefly luciferase in yeast extracts prepared from eL24 control cells (**A**), eB13Δ cells (**B**) or eL24Δ cells (**C**). *In vitro* translation was carried out at 25°C in 30 μl starting volume using 500 ng of mRNA as a template. For each strain at least three independent extracts were analyzed, each extract was analyzed by at least two independent reactions. The average (mean ± SD) relative light units (RLU) of all reactions are plotted. Red dashed-line square marks the areas that were magnified and displayed on the right. TFAs are indicated by arrows. The average (mean ± SD) differences between Renilla and Firefly TFA values across all reactions are presented in minutes.

Further examination of the eB13Δ mutant demonstrated two distinct functions of the eB13 bridge. First, this bridge supports initiation step of translation. Defects in the eB13 bridge lead to accumulation of free subunits and halfmers *in vivo*, and reduction of *in vitro* translation rate (Figures 3A and 6C). In addition, formation of intermediate ribosomal particles *in vitro* points to incorrect subunit interactions due to compromised eB13 bridge (Figure 5). Imperfect subunit joining indicates that eB13 bridge participates in the formation of 80S ribosome at the initiation step of translation. Second, eB13 is important for the elongation step of translation. Ribosomes lacking eB13 bridge have ∼1.3 times reduced rate of *in vitro* elongation compared to control ribosomes (Figure 7). At present, there are no com-

plete high-resolution atomic models of rotational states of yeast ribosome, which could shed light on the role of the eB13 bridge during translation elongation. For that reason electron maps of human ribosomes obtained by cryo-electron microscopy were used to visualize structure of eB13 in rotated and unrotated conformations (10,13). Analysis of linker region of eL24 in both rotational states revealed very low electron density indicating that this region is dynamical. It has been previously suggested that flexible linker region of eL24 follows rotation of 40S subunit (11,54). In contrast, C-terminal α-helical domain (e.g. aa residues R101, R105, K117) have similar interaction interface with small subunit in both rotational states and may act as a tethered anchor (10,13,54). Therefore, eB13 bridge contributes to the ratcheting of the 40S subunit during translocation. Analysis of eukaryotic elongation cycle by cryo-electron microscopy revealed that translocation of the ribosome after peptide bond formation occurs in two main steps. First step involves rotation of the 40S subunit relative to the 60S subunit. This allows tRNA to transit from the canonical P/P and A/A states into the hybrid P/E and A/P states (54,55). Second step requires presence of the elongation factor eEF2. This factor triggers movement of tRNAs from the hybrid P/E and A/P states into the canonical E/E and P/P sites and simultaneous movement of mRNA across the ribosome (54,55). eEF2-dependent step is accompanied by the back-rotation of the 40S subunit relative to the 60S subunit (11,36,54). Interestingly, resent study has revealed the communication pathway between the eEF2 binding site and the 40S subunit through the rearrangement of the eB13 bridge (56). Altogether, reduced elongation rate reflects the involvement of eB13 bridge in the maintenance of ribosome conformation by controlling the ribosome subunit rotation during elongation cycle.

The N-terminal domain of eL24 resides in the 60S subunit and forms universally conserved bridge B6 (Supplementary Figure S1). Results of this study demonstrate that loss of B6 bridge has no apparent influence on the yeast cell growth and global level of translation (Figure 2). Structure of B6 varies significantly among different species and becomes less complex with increasing complexity of ribosome. In the *Escherichia coli* ribosome B6 bridge contains numerous contacts between bacteria specific protein bL19 and helix 44 of 16S rRNA (12). In contrast, in the yeast ribosome B6 bridge consists of only two interactions between R43 and R47 of eL24 and h44 of 18S rRNA (11). In the human ribosome this bridge is reduced to a single R47 residue contacting with h44 (13). There is also a structural evidence that B6 bridge is absent in the post-translocational state of human ribosome (54). Although structure of B6 bridge is known, the role of this bridge in the ribosome remains unresolved.

Intriguingly, analysis of dynamics of *in vitro* translation in cell-free extracts of eL24 mutants suggests the involvement of N-terminal domain of eL24 in the initiation step of translation (Figure 6C). Structural studies of eukaryotic ribosomes revealed that N-terminal domain of eL24 is located close to the binding site for initiation factor eIF5B (34,35). eIF5B is a translational GTPase involved in the last step of translation initiation. At this step eIF5B-GTP stimulates dissociation of eIF2-GDP from the 48S pre-initiation complex after start codon recognition. Subsequently, eIF5B-GTP binds to the pre-initiation complex and facilitates joining of 40S and 60S subunits (14,57,58). eIF5B interacts with sarcin-ricin loop (helix H95) of 28S rRNA and protein uL14. Although N-terminal domain of eL24 do not form direct contact with eIF5B, it interacts with protein uL14 and neighbor helix H96 (34). The binding site for the initiation factor eIF6 (ribosomal anti-association factor) was also located in this region (37,59). eIF6 mainly interacts with protein uL14, however several contacts of eIF6 with N-terminal domain of eL24 were observed (37,59). It has been proposed that eIF6 and the 40S subunit compete for a common region in the 60S subunit and presence of eIF6 prevents formation of the 80S ribosome by steric hindrance (37). Therefore, both eIF5B and eIF6 share closely positioned binding sites and both act at the subunit joining step of initiation, either promoting (eIF5B) or inhibiting it (eIF6) (14,60). It is possible that the N-terminal domain of eL24 allosterically regulates binding sites of eIF5B and/or eIF6 through the interaction with the uL14 protein. Cryo-EM studies of ribosomes from eB13Δ and eL24Δ mutants will show in what manner the N-terminal domain of eL24 coordinates the binding of these factors. Alternatively, eIF5B and eIF6 can affect the conformation of the N-terminal domain of eL24 through the interaction with the uL14. The comparison of the existing structural models of ribosomes with and without these factors did not reveal any changes in the conformations of eL24 and uL14 (11,34–37).

Incorporation of eL24 into 60S subunit occurs at the cytoplasmic step of subunit assembly (22,23). Therefore, eL24 protein can exist in two forms - bound to the ribosome and free in the cytoplasm. It is possible that eL24 may affect translation of specific mRNA while being in one or the other form, which may explain effects of the deletion of eL24. The future studies may reveal the possibility of this regulation.

In conclusion, this study demonstrates pleiotropic functions of different domains of eukaryotic ribosomal protein eL24. Bridge eB13 (via linker region and C-terminal α-helix of eL24) is important for the correct subunit joining during initiation and elongation steps of translation. Functional integrity of this bridge mainly depends on the protein–protein type contacts between eL24 and eS6. Intriguingly, the universal bridge B6 has only a minor role if any. Perhaps the most exciting result obtained here is that the N-terminal domain of eL24 may have a function during translation initiation. It should be noted that structural studies of both yeast and human ribosomes determined another protein, structurally very similar to eL24, named eL19 (11,13). This protein is also composed of three domains. The C-terminal α-helix of eL19 extends from the E- site of ribosome and forms bridge eB12, which has been previously shown to be involved in supporting of ribosomal subunit association. The N-terminal domain and middle region of eL19 are essential for ribosome biogenesis (16). Taken together, structurally similar eL24 and eL19 collectively perform a number of essential for the ribosome functionality tasks regulating ribosome biogenesis, initiation and elongation of translation.

SUPPLEMENTARY DATA

Supplementary Data are available at NAR Online.

ACKNOWLEDGEMENTS

We thank all members of the Chair of Molecular Biology, especially Dr Aivar Liiv and Dr Margus Leppik, for their support and for helpful discussions and Silva Lilleorg and Kaspar Reier for critical reading of the manuscript. We are grateful to Dr Märt Möls for discussions and assistance in analysing of experimental data.

FUNDING

Estonian Ministry of Education and Research (Estonian Research Council Institutional Research Funding) [IUT20-21 to to J.R.]. Funding for open access charge: Estonian Science Council.
Conflict of interest statement. None declared.

REFERENCES

1. Buttgereit,F. and Brand,M.D. (1995) A hierarchy of ATP-consuming processes in mammalian cells. *Biochem.J.*, **312**, 163–167.
2. Warner,J.R. (1999) The economics of ribosome biosynthesis in yeast. *Trends Biochem. Sci.*, **24**, 437–440.
3. Sonenberg,N. and Hinnebusch,A.G. (2009) Regulation of translation initiation in eukaryotes: mechanisms and biological targets. *Cell*, **136**, 731–745.
4. Bhat,M., Robichaud,N., Hulea,L., Sonenberg,N., Pelletier,J. and Topisirovic,I. (2015) Targeting the translation machinery in cancer. *Nat. Rev. Drug Discov.*, **14**, 261–278.
5. Danilova,N. and Gazda,H.T. (2015) Ribosomopathies: how a common root can cause a tree of pathologies. *Dis. Models Mech.*, **8**, 1013–1026.
6. Nakhoul,H., Ke,J., Zhou,X., Liao,W., Zeng,S.X. and Lu,H. (2014) Ribosomopathies: mechanisms of disease. *Clin. Med. Insights. Blood Disord.*, **7**, 7–16.
7. Wang,W., Nag,S., Zhang,X., Wang,M.H., Wang,H., Zhou,J. and Zhang,R. (2015) Ribosomal proteins and human diseases: pathogenesis, molecular mechanisms, and therapeutic implications. *Med. Res. Rev.*, **35**, 225–285.
8. Yusupov,M.M., Yusupova,G.Z., Baucom,A., Lieberman,K., Earnest,T.N., Cate,J.H. and Noller,H.F. (2001) Crystal structure of the ribosome at 5.5 A resolution. *Science*, **292**, 883–896.
9. Zhang,W., Dunkle,J.A. and Cate,J.H. (2009) Structures of the ribosome in intermediate states of ratcheting. *Science*, **325**, 1014–1017.
10. Anger,A.M., Armache,J.P., Berninghausen,O., Habeck,M., Subklewe,M., Wilson,D.N. and Beckmann,R. (2013) Structures of the human and Drosophila 80S ribosome. *Nature*, **497**, 80–85.
11. BenShem,A., Garreau de Loubresse,N., Melnikov,S., Jenner,L., Yusupova,G. and Yusupov,M. (2011) The structure of the eukaryotic ribosome at 3.0 A resolution. *Science*, **334**, 1524–1529.
12. Liu,Q. and Fredrick,K. (2016) Intersubunit bridges of the bacterial ribosome. *J. Mol. Biol.*, **428**, 2146–2164.
13. Khatter,H., Myasnikov,A.G., Natchiar,S.K. and Klaholz,B.P. (2015) Structure of the human 80S ribosome. *Nature*, **520**, 640–645.
14. Dever,T.E., Kinzy,T.G. and Pavitt,G.D. (2016) Mechanism and regulation of protein synthesis in saccharomyces cerevisiae. *Genetics*, **203**, 65–107.
15. Dresios,J., Panopoulos,P., Suzuki,K. and Synetos,D. (2003) A dispensable yeast ribosomal protein optimizes peptidyltransferase activity and affects translocation. *J. Biol. Chem.*, **278**, 3314–3322.
16. Kisly,I., Gulay,S.P., Maeorg,U., Dinman,J.D., Remme,J. and Tamm,T. (2016) The functional role of eL19 and eB12 intersubunit bridge in the eukaryotic ribosome. *J. Mol. Biol.*, **428**, 2203–2216.
17. Meskauskas,A., Harger,J.W., Jacobs,K.L. and Dinman,J.D. (2003) Decreased peptidyltransferase activity correlates with increased programmed 1 ribosomal frameshifting and viral maintenance defects in the yeast Saccharomyces cerevisiae. *RNA*, **9**, 982–992.
18. Steffen,K.K., McCormick,M.A., Pham,K.M., MacKay,V.L., Delaney,J.R., Murakami,C.J., Kaeberlein,M. and Kennedy,B.K. (2012) Ribosome deficiency protects against ER stress in Saccharomyces cerevisiae. *Genetics*, **191**, 107–118.
19. BaronasLowell,D.M. and Warner,J.R. (1990) Ribosomal protein L30 is dispensable in the yeast Saccharomyces cerevisiae. *Mol. Cell. Biol.*, **10**, 5235–5243.
20. Armache,J.P., Anger,A.M., Marquez,V., Franckenberg,S., Frohlich,T., Villa,E., Berninghausen,O., Thomm,M., Arnold,G.J., Beckmann,R. *et al.* (2013) Promiscuous behaviour of archaeal ribosomal proteins: implications for eukaryotic ribosome evolution. *Nucleic Acids Res.*, **41**, 1284–1293.
21. Kappel,L., Loibl,M., Zisser,G., Klein,I., Fruhmann,G., Gruber,C., Unterweger,S., Rechberger,G., Pertschy,B. and Bergler,H. (2012) Rlp24 activates the AAAATPase Drg1 to initiate cytoplasmic pre60S maturation. *J. Cell Biol.*, **199**, 771–782.
22. Konikkat,S. and Woolford,J.L. Jr (2017) Principles of 60S ribosomal subunit assembly emerging from recent studies in yeast. *Biochem. J.*, **474**, 195–214.
23. Saveanu,C., Namane,A., Gleizes,P.E., Lebreton,A., Rousselle,J.C., NoaillacDepeyre,J., Gas,N., Jacquier,A. and FromontRacine,M. (2003) Sequential protein association with nascent 60S ribosomal particles. *Mol. Cell. Biol.*, **23**, 4449–4460.
24. Dresios,J., Derkatch,I.L., Liebman,S.W. and Synetos,D. (2000) Yeast ribosomal protein L24 affects the kinetics of protein synthesis and ribosomal protein L39 improves translational accuracy, while mutants lacking both remain viable. *Biochemistry*, **39**, 7236–7244.
25. Dresios,J., Panopoulos,P., Frantziou,C.P. and Synetos,D. (2001) Yeast ribosomal protein deletion mutants possess altered peptidyltransferase activity and different sensitivity to cycloheximide. *Biochemistry*, **40**, 8101–8108.
26. Sikorski,R.S. and Hieter,P. (1989) A system of shuttle vectors and yeast host strains designed for efficient manipulation of DNA in Saccharomyces cerevisiae. *Genetics*, **122**, 19–27.
27. Knop,M., Siegers,K., Pereira,G., Zachariae,W., Winsor,B., Nasmyth,K. and Schiebel,E. (1999) Epitope tagging of yeast genes using a PCRbased strategy: more tags and improved practical routines. *Yeast*, **15**, 963–972.
28. Sherman,F. (2002) Getting started with yeast. *Methods Enzymol.*, **350**, 3–41.
29. Janke,C., Magiera,M.M., Rathfelder,N., Taxis,C., Reber,S., Maekawa,H., MorenoBorchart,A., Doenges,G., Schwob,E., Schiebel,E. *et al.* (2004) A versatile toolbox for PCR-based tagging of yeast genes: new fluorescent proteins, more markers and promoter substitution cassettes. *Yeast*, **21**, 947–962.
30. Hentges,P., Van Driessche,B., Tafforeau,L., Vandenhaute,J. and Carr,A.M. (2005) Three novel antibiotic marker cassettes for gene disruption and marker switching in Schizosaccharomyces pombe. *Yeast*, **22**, 1013–1019.
31. Rhodin,M.H. and Dinman,J.D. (2010) A flexible loop in yeast ribosomal protein L11 coordinates P-site tRNA binding. *Nucleic Acids Res.*, **38**, 8377–8389.
32. Piir,K., Tamm,T., Kisly,I., Tammsalu,T. and Remme,J. (2014) Stepwise splitting of ribosomal proteins from yeast ribosomes by LiCl. *PLoS One*, **9**, e101561.
33. Cox,J. and Mann,M. (2008) MaxQuant enables high peptide identification rates, individualized p.p.b.-range mass accuracies and proteome-wide protein quantification. *Nat. Biotechnol.*, **26**, 1367–1372.
34. Fernandez,I.S., Bai,X.C., Hussain,T., Kelley,A.C., Lorsch,J.R., Ramakrishnan,V. and Scheres,S.H.W. (2013) Molecular architecture of a eukaryotic translational initiation complex. *Science*, **342**, 1240585.
35. Yamamoto,H., Unbehaun,A., Loerke,J., Behrmann,E., Collier,M., Burger,J., Mielke,T. and Spahn,C.M. (2014) Structure of the mammalian 80S initiation complex with initiation factor 5B on HCV-IRES RNA. *Nat. Struct. Mol. Biol.*, **21**, 721–727.
36. Budkevich,T.V., Giesebrecht,J., Behrmann,E., Loerke,J., Ramrath,D.J., Mielke,T., Ismer,J., Hildebrand,P.W., Tung,C.S., Nierhaus,K.H. *et al.* (2014) Regulation of the mammalian elongation cycle by subunit rolling: a eukaryotic-specific ribosome rearrangement. *Cell*, **158**, 121–131.

37. Gartmann,M., Blau,M., Armache,J.P., Mielke,T., Topf,M. and Beckmann,R. (2010) Mechanism of eIF6-mediated inhibition of ribosomal subunit joining. *J. Biol. Chem.*, **285**, 14848–14851.
38. Iizuka,N. and Sarnow,P. (1997) Translation-competent extracts from Saccharomyces cerevisiae: effects of L-A RNA, 5' cap, and 3' poly(A) tail on translational efficiency of mRNAs. *Methods*, **11**, 353–360.
39. Tarun,S.Z. Jr. and Sachs,A.B. (1995) A common function for mRNA 5' and 3' ends in translation initiation in yeast. *Genes Dev.*, **9**, 2997–3007.
40. Carter,A.P., Clemons,W.M., Brodersen,D.E., Morgan-Warren,R.J., Wimberly,B.T. and Ramakrishnan,V. (2000) Functional insights from the structure of the 30S ribosomal subunit and its interactions with antibiotics. *Nature*, **407**, 340–348.
41. Shah,P., Ding,Y., Niemczyk,M., Kudla,G. and Plotkin,J.B. (2013) Rate-limiting steps in yeast protein translation. *Cell*, **153**, 1589–1601.
42. Wu,S., Tutuncuoglu,B., Yan,K., Brown,H., Zhang,Y., Tan,D., Gamalinda,M., Yuan,Y., Li,Z., Jakovljevic,J. *et al.* (2016) Diverse roles of assembly factors revealed by structures of late nuclear pre-60S ribosomes. *Nature*, **534**, 133–137.
43. Lo,K.Y., Li,Z., Bussiere,C., Bresson,S., Marcotte,E.M. and Johnson,A.W. (2010) Defining the pathway of cytoplasmic maturation of the 60S ribosomal subunit. *Mol. Cell*, **39**, 196–208.
44. Greber,B.J., Boehringer,D., Montellese,C. and Ban,N. (2012) Cryo-EM structures of Arx1 and maturation factors Rei1 and Jjj1 bound to the 60S ribosomal subunit. *Nat. Struct. Mol. Biol.*, **19**, 1228–1233.
45. Kemmler,S., Occhipinti,L., Veisu,M. and Panse,V.G. (2009) Yvh1 is required for a late maturation step in the 60S biogenesis pathway. *J. Cell Biol.*, **186**, 863–880.
46. Weis,F., Giudice,E., Churcher,M., Jin,L., Hilcenko,C., Wong,C.C., Traynor,D., Kay,R.R. and Warren,A.J. (2015) Mechanism of eIF6 release from the nascent 60S ribosomal subunit. *Nat. Struct. Mol. Biol.*, **22**, 914–919.
47. Andersson,S.G. and Kurland,C.G. (1990) Codon preferences in free-living microorganisms. *Microbiol. Rev.*, **54**, 198–210.
48. Arava,Y., Wang,Y., Storey,J.D., Liu,C.L., Brown,P.O. and Herschlag,D. (2003) Genome-wide analysis of mRNA translation profiles in Saccharomyces cerevisiae. *Proc. Natl. Acad. Sci. U.S.A.*, **100**, 3889–3894.
49. Bulmer,M. (1991) The selection-mutation-drift theory of synonymous codon usage. *Genetics*, **129**, 897–907.
50. Kolb,V.A., Makeyev,E.V. and Spirin,A.S. (1994) Folding of firefly luciferase during translation in a cell-free system. *EMBO J.*, **13**, 3631–3637.
51. Jorgensen,F. and Kurland,C.G. (1990) Processivity errors of gene expression in Escherichia coli. *J. Mol. Biol.*, **215**, 511–521.
52. Tsung,K., Inouye,S. and Inouye,M. (1989) Factors affecting the efficiency of protein synthesis in Escherichia coli. Production of a polypeptide of more than 6000 amino acid residues. *J. Biol. Chem.*, **264**, 4428–4433.
53. Meyuhas,O. (2008) Physiological roles of ribosomal protein S6: one of its kind. *Int. Rev. Cell Mol. Biol.*, **268**, 1–37.
54. Behrmann,E., Loerke,J., Budkevich,T.V., Yamamoto,K., Schmidt,A., Penczek,P.A., Vos,M.R., Burger,J., Mielke,T., Scheerer,P. *et al.* (2015) Structural snapshots of actively translating human ribosomes. *Cell*, **161**, 845–857.
55. Dever,T.E. and Green,R. (2012) The elongation, termination, and recycling phases of translation in eukaryotes. *Cold Spring Harbor Perspect. Biol.*, **4**, a013706.
56. Gulay,S.P., Bista,S., Varshney,A., Kirmizialtin,S., Sanbonmatsu,K.Y. and Dinman,J.D. (2017) Tracking fluctuation hotspots on the yeast ribosome through the elongation cycle. *Nucleic Acids Res.*, **45**, 4958–4971.
57. Hinnebusch,A.G. and Lorsch,J.R. (2012) The mechanism of eukaryotic translation initiation: new insights and challenges. *Cold Spring Harbor Perspect.Biol.*, **4**, a011544.
58. Hinnebusch,A.G. (2014) The scanning mechanism of eukaryotic translation initiation. *Annu. Rev. Biochem.*, **83**, 779–812.
59. Klinge,S., Voigts-Hoffmann,F., Leibundgut,M., Arpagaus,S. and Ban,N. (2011) Crystal structure of the eukaryotic 60S ribosomal subunit in complex with initiation factor 6. *Science*, **334**, 941–948.
60. Ceci,M., Gaviraghi,C., Gorrini,C., Sala,L.A., Offenhauser,N., Marchisio,P.C. and Biffo,S. (2003) Release of eIF6 (p27BBP) from the 60S subunit allows 80S ribosome assembly. *Nature*, **426**, 579–584.